
ShrinkTeaNet: Million-scale Lightweight Face Recognition via Shrinking Teacher-Student Networks

Chi Nhan Duong
Concordia University
dcnhan@ieee.org

Khoa Luu
University of Arkansas
khoaluu@uark.edu

Kha Gia Quach
Concordia University
kquach@ieee.org

Ngan Le
Carnegie Mellon University
thihoanl@andrew.cmu.edu

Abstract

Large-scale face recognition in-the-wild has been recently achieved matured performance in many real work applications. However, such systems are built on GPU platforms and mostly deploy heavy deep network architectures. Given a high-performance heavy network as a teacher, this work presents a simple and elegant teacher-student learning paradigm, namely *ShrinkTeaNet*, to train a portable student network that has significantly fewer parameters and competitive accuracy against the teacher network. Far apart from prior teacher-student frameworks mainly focusing on accuracy and compression ratios in closed-set problems, our proposed teacher-student network is proved to be more robust against open-set problem, i.e. large-scale face recognition. In addition, this work introduces a novel Angular Distillation Loss for distilling the feature direction and the sample distributions of the teacher’s hypersphere to its student. Then *ShrinkTeaNet* framework can efficiently guide the student’s learning process with the teacher’s knowledge presented in both intermediate and last stages of the feature embedding. Evaluations on LFW, CFP-FP, AgeDB, IJB-B and IJB-C Janus, and MegaFace with one million distractors have demonstrated the efficiency of the proposed approach to learn robust student networks which have satisfying accuracy and compact sizes. Our *ShrinkTeaNet* is able to support the light-weight architecture achieving high performance with 99.77% on LFW and 95.64% on large-scale Megaface protocols.

1 Introduction

Deep learning has been widely used in many disciplines with remarkable results comparing to previous methods. The idea of deep learning goes back to 1980s but the advent of GPUs in 2000s paved a way for using deep neural network in many areas. The breakthrough is apparent in 2012 ImageNet competition where Krizhevsky et al. presented AlexNet [1] reducing the top-5 error with stunning result comparing the second run up. In recent time, many modern network architectures proposed that improve performance in various domains of computer vision with different applications. VGGNet [2], GoogLeNet [3], ResNet [4] and FishNet [5] are prominent among other neural network architectures. Regardless of the performance improvement, these architectures conduct huge amount of computations. For example, GoogLeNet has 138 million parameters which takes few seconds to run a normal size image. Hence, such kind of networks can only be performed well using special hardware which have the capacity of parallel computing and high performance. On the other hand, such large network architectures cannot be applied on cell phones or embedded devices. Consequently,

Table 1: The comparison of the properties between our distillation approach and other methods. ℓ_{CE} denotes the cross-entropy loss. Feature Distribution (Feat. Dist.), Activation (Act), Gradient (Grad).

Method	Object Class	Teacher Transform	Student Transform	Distilled Knowledge	Loss Function	Missing Info.
KD [7]	Closed-set	Identity	Identity	Logits	ℓ_{CE}	✗
FitNets [8]	Closed-set	Identity	1×1 conv	Magnitude	ℓ_2	✗
Att_Trans[10]	Closed-set	Attention	Attention	Act/Grad Map	ℓ_2	✓
DNN_FSP [9]	Closed-set	Correlation	Correlation	Feat. Flow	ℓ_2	✓
Jacob_Match [13]	Closed-set	Gradient	Gradient	Jacobians	ℓ_2	✓
Factor_Trans [15]	Closed-set	Encoder	Encoder	Feat. Factors	ℓ_1	✓
Act_Bound [11]	Closed-set	Binarization	1×1 conv	Act Map	Marginal ℓ_2	✓
AL_PSN[14]	Closed-set	Identity	Identity	Feat. Dist.	ℓ_{GAN}	✓
Robust SNL[12]	Closed-set	Identity	Identity	Scores + Grad	ℓ_2	✗
Ours	Open-set	Identity	1×1 conv	Direction	Angular	✗

network architectures without requiring high-power machine while retaining similar accuracy are in high demand in mobile devices and embedded application.

In recent years, Knowledge Distillation has become a prominent topic by its ability to transfer the interpretation capability of a heavy network to other light architectures and make them more powerful. Given a heavy but powerful network (i.e. *teacher*), conventional distillation approaches [6, 7] encouraged the similarity between the outputs of an input light-weight network (i.e. *student*) and the teacher network to boost the student’s performance. By this way, the student can efficiently inherit the power and advantages of its teacher. Different metrics have been proposed for the similarity measurements such as ℓ_2 or cross-entropy losses. Some other approaches injected these metrics into middle layers and exploited various aspects of the teacher network such as feature magnitude [8], feature flow [9], activation maps [10, 11], gradient maps [12], and other factors [13–15].

Although these methods have achieved prominent results, most of them are proposed for closed-set problems where the object classes are predefined and remain the same in both training and testing phases. With this assumption, the prediction scores of the teacher can be transferred and used as supervised signals for the student. However, when the classes are different between training and testing (i.e. open-set face recognition), prediction scores of the training classes become less valuable since they are changed during testing phase. As a result, the student may have lots of difficulties when dealing with new classes. Moreover, ℓ_2 loss are usually adopted for either the last output layer or middle layers. This is actually a hard constraint for the student while it leads toward an “exact match” between the features of the two networks. Therefore, when it is adopted to multiple layers, training process of the student network may have the over-regularized issues and become unstable.

Contributions. This paper introduces a novel teacher-student learning algorithm, namely *ShrinkTeaNet*, for the open-set large-scale face recognition. The contributions of this work are three-fold.

- Firstly, rather than emphasizing on an exact match between features, we propose a novel Angular Distillation Loss for distilling the feature directions and the sample distributions from the teacher’s hypersphere to the student. Compared to ℓ_2 loss, the Angular constraint is “softer” and provides the student more flexibility to interpret the information during embedding process. Moreover, inheriting the sample distributions from its teacher can help the student robustly reuse the learned knowledge even when object classes are changed.
- Secondly, we present a new ShrinkTeaNet framework that efficiently distills the teacher’s knowledge in every stage of the feature embedding process.
- Thirdly, the evaluations show improvements in both small-scale and large-scale benchmarks.

To the best of our knowledge, this is one of the first distillation methods to tackle an open-set large-scale recognition problem.

2 Related work

There has been a rising interest in light-weight deep network design mainly in tuning deep neural architectures to strike an optimal balance between accuracy and speed. Besides directly designing new deep network architectures, depending on the motivations and techniques of the proposed frameworks, they can be divided into two different groups, i.e. network pruning and knowledge distillation.

Network Pruning. Network pruning is to analyze and remove the redundancy presented in the heavy network to obtain the light-weight form with comparable accuracy. Generally, the training framework for approaches in this groups consist of three stages, namely (1) train a large (over-parameterized model), (2) prune the trained large model based on some criterions, and (3) fine-tune the pruned model to obtain good performance. There are two categories developed to prune network. The first category is *unstructured pruning methods* that starts from a large, over-parameterized and high performance model. Optimal Brain Damage [16], Optimal brain surgeon [17] are first network pruning methods which are based on Hessian of the loss function. Pruning network by setting to zero the weights below a threshold, without drop of accuracy is proposed by [18] and it then improved by quantizing the weights to 8 bits or less and finally Huffman encoding [19]. Variational Dropout [20] is also adopted by [21] to prune redundant weights. Recently, [22] adopted sparse networks through ℓ_0 -norm regularization based on stochastic gate. In the second category, i.e. *structured pruning methods*, pruning channels is a popular approach. [23] prunes filters based on its next layer by considering filter pruning as an optimization problem. The importance of a filter is calculated its absolute weights is adopted in [24, 25] to determine which channels to retain. Taylor expansion is adopted in [26] to approximate the importance of each channel over the final loss and prune accordingly.

Knowledge Distillation. Rather than trying to “simplify” the computationally expensive deep network as in previous group, the Knowledge Distillation approaches aim at learning a light-weight network (i.e. student) such that it can mimic the behaviors of the heavy one (i.e. teacher). With the useful information from the teacher, the student can learn more efficient and be more “intelligent”. Inspired by this motivation, one of the first knowledge distillation works is introduced by [6] suggesting to minimize the ℓ_2 distance between the extracted features from the last layers of these two networks. Hilton et al. [7] later pointed out that the hidden relationships between the predicted class probabilities from the teacher is also very important and informative for the student. Then, the soft labels generated by teacher model are adopted as the supervision signal in addition to the regular labeled training data during the training phase. In addition to the soft labels as in [7], Romero et al. [8] bridged the middle layers of the student and teacher networks and adopted ℓ_2 loss to further supervised the output of the student. Several aspects and knowledge of the teacher network are also exploited in literature including transferring the feature activation map [11], feature distribution [14], block feature flow [9], Activation-based and Gradient-based Attention Maps [10], Jacobians [13], Unsupervised Feature Factors [15]. Recently, Guo et al. [12] proposed to distill both prediction scores and gradient maps to enhance the student’s robustness against data perturbations. Other knowledge distillation methods [9, 27–31] are also proposed for variety of learning tasks.

3 Proposed method

This section firstly describes a general form of a knowledge distillation problem. Then two important design aspects for the face recognition are considered including (1) *the representation of the distilled knowledge*; and (2) *how to effectively transfer them between teacher and student*. Finally, the ShrinkTeaNet architecture with the Angular Distillation loss are introduced for distillation process.

Let $\mathcal{T} : \mathcal{I} \mapsto \mathcal{Z}$ and $\mathcal{S} : \mathcal{I} \mapsto \mathcal{Z}$ define the mapping functions from image domain \mathcal{I} to a high-level embedding domain. Both functions \mathcal{T} and \mathcal{S} are the composition of n sub-functions \mathcal{T}_i and \mathcal{S}_i as.

$$\begin{aligned}\mathcal{T}(I; \Theta^t) &= [\mathcal{T}_1 \circ \mathcal{T}_2 \circ \dots \circ \mathcal{T}_n](I, \Theta^t) \\ \mathcal{S}(I; \Theta^s) &= [\mathcal{S}_1 \circ \mathcal{S}_2 \circ \dots \circ \mathcal{S}_n](I, \Theta^s)\end{aligned}\tag{1}$$

where I denotes the input image, Θ^t and Θ^s are parameters of \mathcal{T} and \mathcal{S} , respectively. Then given a *complicated high-capacity function* \mathcal{T} (i.e. *teacher*), the goal of model distillation is to distill the knowledge from \mathcal{T} to a *limited-capacity function* \mathcal{S} (i.e. *student*) so that \mathcal{S} can embed similar latent domain as \mathcal{T} . In order to achieve this goal, the learning process of \mathcal{S} is usually taken place under the supervision of \mathcal{T} by comparing the their outputs step-by-step.

$$\begin{aligned}\mathcal{L}_i(\mathcal{S}, \mathcal{T}) &= d(\mathcal{G}_i^t(F_i^t), \mathcal{G}_i^s(F_i^s)), i = 1..n \\ F_i^t &= [\mathcal{T}_1 \circ \mathcal{T}_2 \circ \dots \circ \mathcal{T}_i](I, \Theta^t) \\ F_i^s &= [\mathcal{S}_1 \circ \mathcal{S}_2 \circ \dots \circ \mathcal{S}_i](I, \Theta^s)\end{aligned}\tag{2}$$

where $\mathcal{G}_i^t(\cdot)$ and $\mathcal{G}_i^s(\cdot)$ are transformation functions of \mathcal{T} and \mathcal{S} making their corresponding embedded features comparable. $d(\cdot, \cdot)$ denotes the difference between these transformed features. Then by minimizing these differences $\mathcal{L}_{distill} = \sum_i^n \lambda_i \mathcal{L}_i(\mathcal{S}, \mathcal{T})$, the knowledge from the teacher \mathcal{T} can be

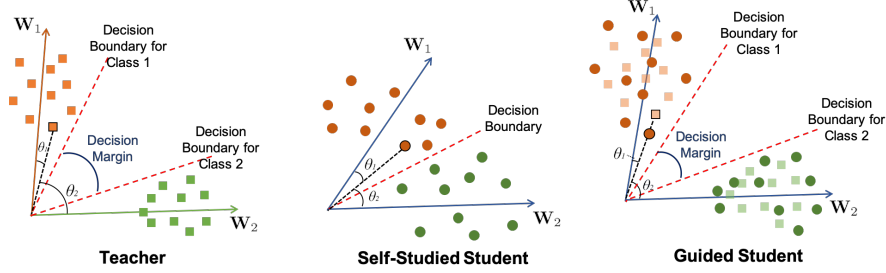


Figure 1: **Geometric Interpretation of Angular Distillation Loss.** With high-capacity function \mathcal{T} , the teacher is able to produce a large decision margin between two classes while the self-studied student only gives small decision margin. By following the direction provided by the teacher, the student can make better decision boundaries with larger margin between classes. Moreover, with the angular distillation loss, the student is not strictly required to produce exact feature as its teacher (*i.e. which is a very hard constraint according to the student’s capability*).

transferred to the student \mathcal{S} so that they can embed similar latent domain. It is worth noting that the form of $\mathcal{L}_i(\mathcal{S}, \mathcal{T})$ provides two important properties. Firstly, since $d(\cdot, \cdot)$ measures the distance between F_i^t and F_i^s , it implicitly defines the knowledge to be transferred from \mathcal{T} to \mathcal{S} . Secondly, the transformation functions $\mathcal{G}_i^t(\cdot)$ and $\mathcal{G}_i^s(\cdot)$ controls the portion of the transferred information. The next sections focus on the designs of these two components for selecting the most useful information and transferring them to the student without missing important information from the teacher.

3.1 Distilled Knowledge from Teacher Hypersphere

As presented in Table 1, most previous distillation frameworks are introduced for the closed set classification problem, *i.e.* object classification or semantic segmentation with predefined classes. With the assumption about the fixed (and small) number of classes, traditional metrics can be efficiently adopted for distillation process. For example, the ℓ_2 distance can be used for similarity measurement between \mathcal{S} and \mathcal{T} , *i.e.* $d(\mathcal{G}_i^t(F_i^t), \mathcal{G}_i^s(F_i^s)) = \|\mathcal{G}_i^t(F_i^t) - \mathcal{G}_i^s(F_i^s)\|_2^2$. However, since the capacity of \mathcal{S} is limited, employing this constraint as a regularization to each F_i^s (*i.e.* to enforce F_i^s and F_i^t to be exact matched) can lead to the over-regularized issue. Consequently, this constraint becomes too hard and makes the learning process of \mathcal{S} more difficult. Another metric is to adopt the class probabilities predicted from the teacher \mathcal{T} as the soft target distribution for the student \mathcal{S} [7]. However, this metric is efficient only when the object classes are fixed in both training and testing phases. Otherwise, the knowledge to convert embedded features to class probabilities cannot be reused during testing stage and, therefore, the distilled knowledge is also partially ignored.

In open-set problems, since classes are not predefined beforehand, the sample distributions of each class and the margin between classes become more valuable knowledge. In other words, with the open-set problems, the angular differences between samples and how the samples distributed in the teacher’s hypersphere are more beneficial for the student. Therefore, we propose to use the angular information as the main knowledge to be distilled. By this way, rather than enforcing the student follow the exact outputs of the teacher (as in case of ℓ_2 distance), we can relax the constraint so that the embedded features extracted by the student only need to have similar direction as those extracted by the teacher. Generally, with “softer” the distillation constraint, the student is able to adaptively interpret the teacher’s information and learn the solution process more efficiently.

Softmax Loss Revisit. As one of the most widely used losses for classification problem, Softmax loss of each input image is formulated as follows.

$$\mathcal{L}_{SM} = -\log \frac{e^{\mathbf{W}_y * F_n^s}}{\sum_{c=1}^C e^{\mathbf{W}_c * F_n^s}} = -\log \frac{e^{\|\mathbf{W}_y\| \|F_n^s\| \cos \theta_y}}{\sum_{c=1}^C e^{\|\mathbf{W}_c\| \|F_n^s\| \cos \theta_c}} \quad (3)$$

where y is the index of the correct class of the input image and C denotes the number of classes. Notice that the bias term is fixed to 0 for simplicity. By adopting the ℓ_2 normalisation to both feature F_n^s and weight \mathbf{W}_c , the angle between them becomes the only classification criteria. If each weight vector \mathbf{W}_c is regarded as the representative of class c , minimizing the loss means that the samples of each class are required to distributed around that class’ representative with the minimal angular difference. This is also true during testing process where the angle between the direction of

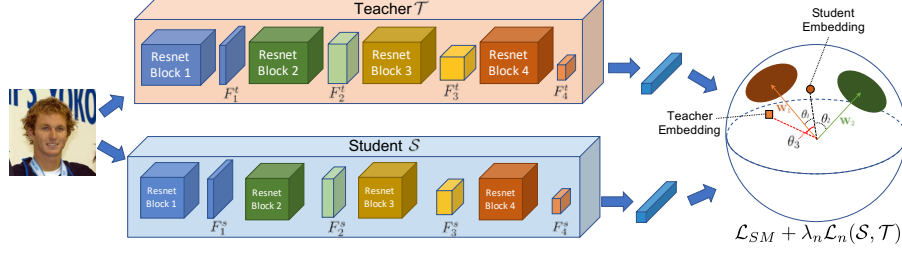


Figure 2: **ShrinkTeaNet Architecture For Knowledge Distillation in Last Layer.** Given an input image, the feature directions provided by the student is optimized using both directions of the class’ representative and the teacher embedding.

extracted features from input image and the representative of each class (i.e. classification problem with predefined classes) or extracted features of other sample (i.e. verification problem) are used for deciding whether they belong to the same class. In this respect, the magnitude of the feature F_n^s becomes less important than its direction. Therefore, rather than considering both magnitude and direction of F_n^t for distillation process, knowledge about the direction is enough for the student to achieve similar distribution as the teacher’s hypersphere. Moreover, this knowledge can be also efficiently reused to compare samples of object classes other than the ones in training.

Feature Direction as Distilled Knowledge. We propose to use the direction of the teacher feature F_n^t as the distilled knowledge and define an **angular distillation loss** as follows.

$$\mathcal{L}_n(\mathcal{S}, \mathcal{T}) = d(\mathcal{G}_n^t(F_n^t), \mathcal{G}_n^s(F_n^s)) = \left\| 1 - \frac{\mathcal{G}_n^t(F_n^t)}{\|\mathcal{G}_n^t(F_n^t)\|} * \frac{\mathcal{G}_n^s(F_n^s)}{\|\mathcal{G}_n^s(F_n^s)\|} \right\|_2^2 \quad (4)$$

With this form of distillation, the only knowledge needed to be transferred between \mathcal{T} and \mathcal{S} is the direction of embedded features. In other words, as long as F_n^s and F_n^t have similar direction, these features can freely distributed on different hyperspheres with various radius in latent space. This produces a degree of freedom for \mathcal{S} to interpret its teacher’s knowledge during learning process. Incorporating this distillation loss to Eqn. (3), the objective function becomes.

$$\mathcal{L} = \mathcal{L}_{SM} + \lambda_n \mathcal{L}_n(\mathcal{S}, \mathcal{T}) \quad (5)$$

The first term corresponds to the traditional classification loss whereas the second term guides the student to learn from the hypersphere of the teacher. Notice that, this objective function is not limited to specific classification loss. This distillation loss can act as a support to any other loss functions.

The Transformation Functions. To prevent missing information during distillation, we choose identity transformation for \mathcal{T} , i.e. $\mathcal{G}_n^t(F_n^t) = F_n^t$, while $\mathcal{G}_n^s(F_n^s)$ is chosen as a mapping function $\mathcal{H}_n^s : \mathbb{R}^{h_n \times w_n \times m_n^s} \mapsto \mathbb{R}^{h_n \times w_n \times m_n^t}$ such that the dimension of F_n^s is increased to match the dimension of F_n^t . For example, if $F_n^s \in \mathbb{R}^{h_n \times w_n \times m_n^s}$ is a feature map extracted from a Deep Neural Network, $\mathcal{H}_n^s(F_n^s)$ can be defined as an 1×1 convolution layer to transform F_n^s to $\bar{F}_n^s \in \mathbb{R}^{h_n \times w_n \times m_n^t}$ where $h_n \times w_n \times m_n^t$ is the dimension of F_n^t . By this way, no information is missing during feature transformation and, therefore, \mathcal{S} can take full advantages of all knowledge from \mathcal{T} .

Geometric Interpretation. Considering the binary classification where there are only two classes with the representatives \mathbf{W}_1 and \mathbf{W}_2 . As presented in previous section, when both embedded features and the representatives are normalized, the classification results depend entirely on the angle between them, i.e. θ_1 and θ_2 . In the training stage, the softmax loss \mathcal{L}_{SM} requires $\theta_1 < \theta_2$ to classify an input image as class 1 and vice versa. As illustrated in Figure 1, with higher capacity, the teacher can provide better decision margin between the two classes, while the self-studied student (i.e. using only softmax loss function) can only give small decision margin. When the $\mathcal{L}_n(\mathcal{S}, \mathcal{T})$ is incorporated (i.e. guided student), the classification margin between class 1 and class 2 is further enhanced by following the feature directions of its teacher and produces better decision boundaries. Furthermore, one can easily see that even when the student is not able to produce exact features as its teacher, it can easily mimic the teacher’s feature directions and be beneficial from the teacher’s hypersphere.

3.2 Intermediate Distilled Knowledge

In this section, we further distill the knowledge of the teacher to intermediate components of the student. Generally, if the input to \mathcal{S} is interpreted as the question and the distribution of its embedded

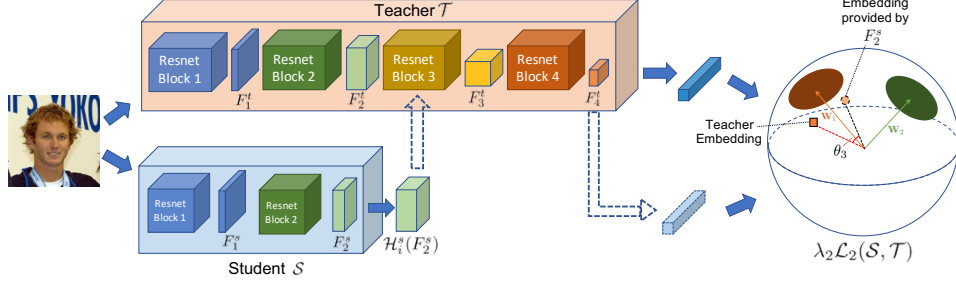


Figure 3: **ShrinkTeaNet Architecture for Intermediate Knowledge Distillation.** Given an intermediate student’s features, i.e. $\mathcal{H}_i^s(F_i^s)$, the teacher use its power to validate whether the student’s input is informative enough to make similar decision as the teacher.

features is its answer, the generated features at the middle stage, i.e. F_i^s , can be viewed as the intermediate understanding or interpretation of the student about the solution process. Then to help the student efficiently “understand” the development of the solution, the teacher should illustrate to the student “*how the good features look like*” and “*whether the current features of the student is good enough to get the solution in later steps*”. Then, the teacher can supervise and efficiently correct the student from the beginning and, therefore, leading to more efficient learning process of the student.

Similar to previous section, rather than employing ℓ_2 norm as the cost function of each pair $\{F_i^s, F_i^t\}$, we proposed to validate the quality of F_i^s based on its angular difference between the embedding produced by F_i^s and F_i^t using the same teacher’s interpretation toward the last stages. In particular, the distillation loss for each intermediate feature F_i^s can be formulated as follows.

$$\begin{aligned}
 \mathcal{L}_i(S, T) &= d(\mathcal{G}_i^t(F_i^t), \mathcal{G}_i^s(F_i^s)) \\
 &= d([\mathcal{T}_{i+1} \circ \dots \circ \mathcal{T}_n](F_i^t), [\mathcal{H}_i^s \circ \mathcal{T}_{i+1} \circ \dots \circ \mathcal{T}_n](F_i^s)) \\
 &= \left\| 1 - \frac{[\mathcal{T}_{i+1} \circ \dots \circ \mathcal{T}_n](F_i^t)}{\|[\mathcal{T}_{i+1} \circ \dots \circ \mathcal{T}_n](F_i^t)\|} * \frac{[\mathcal{H}_i^s \circ \mathcal{T}_{i+1} \circ \dots \circ \mathcal{T}_n](F_i^s)}{\|[\mathcal{H}_i^s \circ \mathcal{T}_{i+1} \circ \dots \circ \mathcal{T}_n](F_i^s)\|} \right\|_2^2
 \end{aligned} \tag{6}$$

The intuition behind this distillation loss for each intermediate feature F_i^s is to validate whether F_i^s contains enough useful information to make the similar decision as its teacher in the later steps. In order to validate this point, we propose to take advantage of the teacher power to solve the solution given the student input at i -th stage, i.e. F_i^s . In case the teacher can still get similar solution using that input, then the student’s understanding until that stage is acceptable. Otherwise, the student is required to be re-corrected immediately. As a result, given the intermediate feature F_i^s , it is firstly transformed by \mathcal{H}_i^s to match the dimension of the teacher feature F_i^t . Then both F_i^s and F_i^t are analyzed by the teacher \mathcal{T} , i.e. $[\mathcal{T}_{i+1} \circ \dots \circ \mathcal{T}_n]$, for the final embedding features. Finally, their similarity in the hypersphere is used for validate the knowledge that F_i^s embeds.

3.3 Shrinking Teacher-Student Network for Face Recognition

Figures 2 and 3 illustrate our proposed ShrinkTeaNet framework to distill the knowledge for both final and intermediate features. Resnet-style convolution neural networks (CNN) with four resnet blocks are adopted for both teacher and student. The whole networks can be considered as the mapping functions, i.e. \mathcal{T} and \mathcal{S} , whereas each resnet block corresponds to each sub-function, i.e. \mathcal{T}_i and \mathcal{S}_i . Then we learn strong but efficient student network by distilling the knowledge to all four blocks. Given the dataset $D = \{I_j, y_j\}_{j=1}^N$ consisting of N facial images I_j and their corresponding labels y_j . The overall learning objective can be formulated as the composition of Eqns. (5) and (6).

$$\mathcal{L} = \frac{1}{N} \sum_j \left[\mathcal{L}_{SM} + \sum_{i=1}^n \lambda_i \mathcal{L}_i(S, T) \right] \tag{7}$$

where λ_i denotes the hyper-parameter control the balance between the distilled knowledge to be transferred at different resnet blocks. Moreover, as presented in previous section, the identity transformation function is used for all functions \mathcal{G}_i^t while 1×1 convolution followed by batch normalization layer is adopted for \mathcal{G}_i^s to match the dimension of the corresponding teacher’s features.

Table 2: Verification performance (%) on different small-scale datasets, i.e. LFW, CFP-FP, AgeDB.

Backbone	# of params	Ratio	Model Type	LFW	CFP-FP	AgeDB
ResNet90 [4]	63.67M	100%	Teacher	99.82%	96.83%	98.37%
MobileNetV1 [32] (MV1)	3.53M	5.54%	Self-Studied	99.53%	93.81%	96.30%
			Student-1 (ℓ_2 loss)	99.60%	93.39%	96.83%
			ShrinkTeaNet-MV1	99.63%	94.23%	97.10%
MobileNetV2 [33] (MV2)	2.15M	3.38%	Self-Studied	99.42%	91.67%	95.28%
			Student-1 (ℓ_2 loss)	99.53%	91.03%	96.20%
			ShrinkTeaNet-MV2	99.63%	93.29%	97.00%
MobileFacenet [34] (MFN)	1.2M	1.88%	Self-Studied	99.45%	92.11%	96.17%
			Student-1 (ℓ_2 loss)	99.50%	91.93%	96.45%
			ShrinkTeaNet-MFN	99.60%	93.44%	96.73%
MobileFacenet-R (MFNR)	3.73M	5.86%	Self-Studied	99.60%	93.80%	96.90%
			Student-1 (ℓ_2 loss)	99.68%	94.51%	97.48%
			ShrinkTeaNet-MFNR	99.77%	95.14%	97.63%

4 Experimental results

4.1 Databases

MS-Celeb-1M [43] consists of 10M photos of 100K subjects. However, a large portion of this dataset includes noisy images or incorrect ID labels. A cleaned version of this dataset [42] is provided with 5.8M photos from 85K identities.

Labeled Faces in the Wild (LFW) [44] is introduced with 13,233 in-the-wild facial images of 5749 subjects. They are divided into 6000 matching pairs with 3000 positive matches.

MegaFace [45] provides a very challenging testing protocol with million-scale of distractors. The gallery set includes more than 1 million images of 690K subjects while the probe set consists of 100K photos from 530 identities.

Celebrities Frontal-Profile [46] was released to validate the models on frontal vs profile modes. It consists of 7000 matching pairs from 500 subjects.

AgeDB [47] provides a protocol with 4 testing age groups where each group consists of 10 splits of 600 matching pairs from 440 subjects. Besides age factor, other facial variations (i.e. pose, illumination, expression) are also included.

IJB-B [48] and **IJB-C** [49] are introduced as two large-scale face verification protocols. While IJB-B provides 12115 templates with 10270 positive matches and 8M negative matches, its extension, i.e. IJB-C, further provides 23124 templates with 19557 positive and 15639K negative matching pairs.

4.2 Implementation Details

Data Preprocessing. All faces are firstly detected using MTCNN [50] and aligned to a predefined template using similarity transformation. They are then cropped to the size of 112×112 .

Network Architectures. For all the experiments, we use the Resnet-90 structure [4] as the teacher network, while different light-weight networks, i.e. MobileNetV1 [32], MobileNetV2 [33], MobileFaceNet [34]. A modified version of MobileFacenet, namely MobileFacenet-R, is also adopted for the student network. This modified version is similar to MobileFacenet except the feature size of each resnet-block is equal to the size of its corresponding features in the teacher network.

Model Configurations. In training stage, the batch size is set to 512. The learning rate starts from 0.1 and the momentum is 0.9. All the models are trained in MXNET environment with a machine of Core i7-6850K @3.6GHz CPU, 64.00 GB RAM with four P6000 GPUs. The λ_n is experimentally

Table 3: Verification performance (%) on LFW.

Method	Training Data	Accuracy
Center Loss [35]	0.7M	99.28%
Sphereface [36]	0.5M	99.42%
Sphereface+ [37]	0.5M	99.47%
Deep-ID2+ [38]	0.3M	99.47%
Marginal Loss [39]	4M	99.48%
RangeLoss [40]	5M	99.52%
FaceNet [41]	200M	99.63%
CosFace [39]	5M	99.73%
ArcFace [42]	5.8M	99.83%
ShrinkTeaNet-MV1	5.8M	99.63%
ShrinkTeaNet-MV2	5.8M	99.63%
ShrinkTeaNet-MFN	5.8M	99.60%
ShrinkTeaNet-MFNR	5.8M	99.77%

Table 4: Comparison with different methods on Megaface Challenge 1 protocol.

Method	Protocol	Accuracy
Sphereface [36]	Small	72.73%
Sphereface+ [37]	Small	73.03%
Center Loss [35]	Small	65.49%
FaceNet [41]	Large	70.49%
CosFace [39]	Large	82.72%
ArcFace [42]	Large	98.35%*
MV1 [32]	Large	91.93%*
ShrinkTeaNet-MV1	Large	94.16%*
MV2 [33]	Large	89.22%*
ShrinkTeaNet-MV2	Large	92.86%*
MFN [34]	Large	89.32%*
ShrinkTeaNet-MFN	Large	91.89%*
MFNR	Large	93.74%*
ShrinkTeaNet-MFNR	Large	95.64%*

Table 5: Comparison with different methods on 1:1 IJB-B and IJB-C Verification protocol. The accuracy is reported at TAR (@FAR=1e-4).

Method	Training Data	IJB-B	IJB-C
SENet50 [51]	VGG2	0.800	0.840
MN-VC [52]	VGG2	0.831	0.862
ResNet50 + DCN [53]	VGG2	0.841	0.880
ArcFace [42]	VGG2	0.898	0.921
ArcFace [42]	MS1M	0.942	0.956
MV1 [32]	MS1M	0.909	0.930
ShrinkTeaNet-MV1	MS1M	0.915	0.936
MV2 [33]	MS1M	0.883	0.907
ShrinkTeaNet-MV2	MS1M	0.902	0.922
MFN [34]	MS1M	0.896	0.918
ShrinkTeaNet-MFN	MS1M	0.898	0.921
MFNR	MS1M	0.912	0.916
ShrinkTeaNet-MFNR	MS1M	0.923	0.940

set to 1 in case of Angular Distillation Loss while this parameter is set to 0.001 as the case of ℓ_2 loss due to the large value of the loss with large feature map. For the intermediate layers, $\lambda_i = \frac{\lambda_{i+1}}{2}$.

4.3 Evaluation Results

Small-scale Protocols. We validate the efficiency of our ShrinkTeaNet framework with four light-weight backbones on small scale protocols. The Resnet-90 trained on MS-Celeb-1M acts as the teacher network. Then, for each light-weight backbone, three cases are considered: (1) Self-studied student which is trained without the help from the teacher; (2) Student-1 which is trained using the objective function as Eqn. (7) but the ℓ_2 function is adopted for distillation loss; and (3) our ShrinkTeaNet with Angular Distillation loss. Table 2 illustrates the performance of the teacher network together with its students. Due to the limited-capacity of the light-weight backbones, in all four cases, the self-studied networks leave the performance gaps of 0.2% – 0.4%, 3.02% – 5.16%, and 1.47% – 3.09% with their teacher on LFW, CFP-FP, and AgeDB, respectively. Although the guided students using ℓ_2 loss can slightly improve the accuracy, it is not always the case when the accuracy of MobileNetV1, MobileNetV2, and MobileFacenet are reduced in CFP-FP benchmark. Moreover, we also notice that the training process with ℓ_2 loss is unstable. Meanwhile, our proposed ShrinkTeaNet efficiently distills the knowledge from the teacher network to its student with the best performance gaps that are significantly reduced to only 0.05%, 1.83%, and 0.74% on the three benchmarks LFW, CFP-FP, AgeDB, respectively. The comparisons with other face recognition methods against LFW are presented in Table 3. From these results, even with the light-weight backbone, ShrinkTeaNet can achieve competitive performance with other large-scale networks.

Megaface Protocol. We adopt similar training process as in small-scale protocols and evaluate our ShrinkTeaNet on the challenging Megaface benchmark against millions of distractors. The comparison in terms of the Rank-1 identification rates between our ShrinkTeaNet and other models is presented in Table 4. These results again show the advantages of our ShrinkTeaNet with consistent improvements provided to the four light-weight student networks. The performance gains for the MV1, MV2, MFN, and MFNR are 2.23%, 3.64%, 2.57%, and 1.9%, respectively. Moreover, the ShrinkTeaNet-MFNR achieves competitive accuracy (i.e. 95.64%) with other large-scale network and reduces the gap with ArcFace [42] to only 1.71%.

IJB-B and IJB-C Protocols. The comparisons against other recent methods on IJB-B and IJB-C benchmarks are also illustrated in Table 5. Similar to the Megaface protocols, ShrinkTeaNet is able to boost the performance of the light-weight backbones significantly and reduce the performance gap to the large-scale backbone to only 0.019 on IJB-B and 0.016 on IJB-C. These results have further emphasized the advantages of the proposed ShrinkTeaNet framework for model distillation.

Conclusions. This paper presents a novel teacher-student learning paradigm, namely ShrinkTeaNet, for open-set face recognition. By adopting the proposed Angular Distillation Loss with the distillation

*refers to the accuracy obtained by using the refined testing dataset with cleaned labels from [42].

on every stage of feature embedding process, the student network can absorb the knowledge of the teacher’s hypersphere in an relaxing and efficient manners. These learned knowledge can flexible adopt even when the testing classes are different from the training ones. Evaluation in both small-scale and large-scale protocols showed the advantages of the proposed ShrinkTeaNet framework.

References

- [1] A. Krizhevsky, I. Sutskever, and G. E. Hinton. Imagenet classification with deep convolutional neural networks. In *Advances in neural information processing systems*, 2012.
- [2] Karen Simonyan and Andrew Zisserman. Very deep convolutional networks for large-scale image recognition. *arXiv preprint arXiv:1409.1556*, 2014.
- [3] Christian Szegedy, Vincent Vanhoucke, Sergey Ioffe, Jon Shlens, and Zbigniew Wojna. Rethinking the inception architecture for computer vision. In *The IEEE Conference on Computer Vision and Pattern Recognition (CVPR)*, June 2016.
- [4] Kaiming He, Xiangyu Zhang, Shaoqing Ren, and Jian Sun. Deep residual learning for image recognition. In *Proceedings of the IEEE conference on computer vision and pattern recognition*, pages 770–778, 2016.
- [5] Shuyang Sun, Jiangmiao Pang, Jianping Shi, Shuai Yi, and Wanli Ouyang. Fishnet: A versatile backbone for image, region, and pixel level prediction. In *Advances in Neural Information Processing Systems*, pages 760–770, 2018.
- [6] J. Ba and R. Caruana. Do deep nets really need to be deep? In *Advances in Neural Information Processing Systems*, 2013.
- [7] Geoffrey E. Hinton, Oriol Vinyals, and Jeffrey Dean. Distilling the knowledge in a neural network. *CoRR*, abs/1503.02531, 2015.
- [8] Adriana Romero, Nicolas Ballas, Samira Ebrahimi Kahou, Antoine Chassang, Carlo Gatta, and Yoshua Bengio. Fitnets: Hints for thin deep nets. In *3rd International Conference on Learning Representations, ICLR 2015, San Diego, CA, USA, May 7-9, 2015, Conference Track Proceedings*, 2015.
- [9] Junho Yim, Donggyu Joo, Jihoon Bae, and Junmo Kim. A gift from knowledge distillation: Fast optimization, network minimization and transfer learning. In *The IEEE Conference on Computer Vision and Pattern Recognition (CVPR)*, July 2017.
- [10] Sergey Zagoruyko and Nikos Komodakis. Paying more attention to attention: Improving the performance of convolutional neural networks via attention transfer. In *5th International Conference on Learning Representations, ICLR 2017, Toulon, France, April 24-26, 2017, Conference Track Proceedings*, 2017.
- [11] Byeongho Heo, Minsik Lee, Sangdoon Yun, and Jin Young Choi. Knowledge transfer via distillation of activation boundaries formed by hidden neurons. *CoRR*, abs/1811.03233, 2018.
- [12] Shiyi He Boxin Shi Chao Xu Dacheng Tao Tianyu Guo, Chang Xu. Robust student network learning. In *The IEEE Conference on Computer Vision and Pattern Recognition (CVPR)*, 2018.
- [13] Suraj Srinivas and François Fleuret. Knowledge transfer with jacobian matching. In *ICML*, volume 80 of *Proceedings of Machine Learning Research*, pages 4730–4738. PMLR, 2018.
- [14] Yunhe Wang, Chang Xu, Chao Xu, and Dacheng Tao. Adversarial learning of portable student networks. In *Thirty-Second AAAI Conference on Artificial Intelligence*, 2018.
- [15] Jangho Kim, Seonguk Park, and Nojun Kwak. Paraphrasing complex network: Network compression via factor transfer. In *Advances in Neural Information Processing Systems 31: Annual Conference on Neural Information Processing Systems 2018, NeurIPS 2018, 3-8 December 2018, Montréal, Canada.*, pages 2765–2774, 2018.
- [16] Yann Le Cun, John S. Denker, and Sara A. Solla. Optimal brain damage. In *Advances in Neural Information Processing Systems*, pages 598–605. Morgan Kaufmann, 1990.
- [17] Babak Hassibi, David G. Stork, Gregory Wolff, and Takahiro Watanabe. Optimal brain surgeon: Extensions and performance comparisons. In *Proceedings of the 6th International Conference on Neural Information Processing Systems, NIPS’93*, pages 263–270, 1993.
- [18] Song Han, Jeff Pool, John Tran, and William J. Dally. Learning both weights and connections for efficient neural network. In *NIPS*, pages 1135–1143, 2015.

- [19] Song Han, Huizi Mao, and William J. Dally. Deep compression: Compressing deep neural network with pruning, trained quantization and huffman coding. In *ICLR*, 2016.
- [20] Diederik P. Kingma, Tim Salimans, and Max Welling. Variational dropout and the local reparameterization trick. *CoRR*, abs/1506.02557, 2015.
- [21] Dmitry Molchanov, Arsenii Ashukha, and Dmitry Vetrov. Variational dropout sparsifies deep neural networks. In *Proceedings of the 34th International Conference on Machine Learning - Volume 70*, pages 2498–2507, 2017.
- [22] Christos Louizos, Max Welling, and Diederik P. Kingma. Learning sparse neural networks through l₀ regularization. In *ICLR*, 2018.
- [23] Jian-Hao Luo, Jianxin Wu, and Weiyao Lin. Thinet: A filter level pruning method for deep neural network compression. In *ICCV*, pages 5068–5076.
- [24] Hao Li, Asim Kadav, Igor Durdanovic, Hanan Samet, and Hans Peter Graf. Pruning filters for efficient convnets. In *ICLR*.
- [25] Ruichi Yu, Ang Li, Chun-Fu Chen, Jui-Hsin Lai, Vlad I. Morariu, Xintong Han, Mingfei Gao, Ching-Yung Lin, and Larry S. Davis. Nisp: Pruning networks using neuron importance score propagation. In *The IEEE Conference on Computer Vision and Pattern Recognition (CVPR)*, June 2018.
- [26] Pavlo Molchanov, Stephen Tyree, Tero Karras, Timo Aila, and Jan Kautz. Pruning convolutional neural networks for resource efficient inference. In *5th International Conference on Learning Representations, ICLR 2017, Toulon, France, April 24-26, 2017, Conference Track Proceedings*, 2017.
- [27] Tommaso Furlanello, Zachary C. Lipton, Michael Tschannen, Laurent Itti, and Anima Anandkumar. Born again neural networks. *CoRR*, abs/1805.04770, 2018.
- [28] Ying Zhang, Tao Xiang, Timothy M. Hospedales, and Huchuan Lu. Deep mutual learning. In *2018 IEEE Conference on Computer Vision and Pattern Recognition, CVPR 2018, Salt Lake City, UT, USA, June 18-22, 2018*, pages 4320–4328, 2018.
- [29] Seyed-Iman Mirzadeh, Mehrdad Farajtabar, Ang Li, and Hassan Ghasemzadeh. Improved knowledge distillation via teacher assistant: Bridging the gap between student and teacher. *CoRR*, abs/1902.03393, 2019.
- [30] Guobin Chen, Wongun Choi, Xiang Yu, Tony Han, and Manmohan Chandraker. Learning efficient object detection models with knowledge distillation. In *In Neural Information Processing Systems*, Long Beach, CA, 2017.
- [31] Xiaojie Wang, Rui Zhang, Yu Sun, and Jianzhong Qi. KDGAN: knowledge distillation with generative adversarial networks. In *Advances in Neural Information Processing Systems 31: Annual Conference on Neural Information Processing Systems 2018, NeurIPS 2018, 3-8 December 2018, Montréal, Canada.*, pages 783–794, 2018.
- [32] Andrew G Howard, Menglong Zhu, Bo Chen, Dmitry Kalenichenko, Weijun Wang, Tobias Weyand, Marco Andreetto, and Hartwig Adam. Mobilenets: Efficient convolutional neural networks for mobile vision applications. *arXiv preprint arXiv:1704.04861*, 2017.
- [33] Mark Sandler, Andrew Howard, Menglong Zhu, Andrey Zhmoginov, and Liang-Chieh Chen. Mobilenetv2: Inverted residuals and linear bottlenecks. In *Proceedings of the IEEE Conference on Computer Vision and Pattern Recognition*, pages 4510–4520, 2018.
- [34] Sheng Chen, Yang Liu, Xiang Gao, and Zhen Han. Mobilefacenets: Efficient cnns for accurate real-time face verification on mobile devices. In *Chinese Conference on Biometric Recognition*, pages 428–438, 2018.
- [35] Yandong Wen, Kaipeng Zhang, Zhifeng Li, and Yu Qiao. A discriminative feature learning approach for deep face recognition. In *European Conference on Computer Vision*, pages 499–515. Springer, 2016.
- [36] Weiyang Liu, Yandong Wen, Zhiding Yu, Ming Li, Bhiksha Raj, and Le Song. Spheraface: Deep hypersphere embedding for face recognition. In *The IEEE Conference on Computer Vision and Pattern Recognition (CVPR)*, volume 1, page 1, 2017.
- [37] Weiyang Liu, Rongmei Lin, Zhen Liu, Lixin Liu, Zhiding Yu, Bo Dai, and Le Song. Learning towards minimum hyperspherical energy. In *Advances in Neural Information Processing Systems*, pages 6222–6233, 2018.

- [38] Yi Sun, Yuheng Chen, Xiaogang Wang, and Xiaoou Tang. Deep learning face representation by joint identification-verification. In *Advances in neural information processing systems*, pages 1988–1996, 2014.
- [39] Hao Wang, Yitong Wang, Zheng Zhou, Xing Ji, Dihong Gong, Jingchao Zhou, Zhifeng Li, and Wei Liu. Cosface: Large margin cosine loss for deep face recognition. In *The IEEE Conference on Computer Vision and Pattern Recognition (CVPR)*, June 2018.
- [40] Xiao Zhang, Zhiyuan Fang, Yandong Wen, Zhifeng Li, and Yu Qiao. Range loss for deep face recognition with long-tailed training data. In *Proceedings of the IEEE Conference on Computer Vision and Pattern Recognition*, pages 5409–5418, 2017.
- [41] Florian Schroff, Dmitry Kalenichenko, and James Philbin. Facenet: A unified embedding for face recognition and clustering. In *Proceedings of the IEEE conference on computer vision and pattern recognition*, pages 815–823, 2015.
- [42] Jiankang Deng, Jia Guo, Xue Niannan, and Stefanos Zafeiriou. Arcface: Additive angular margin loss for deep face recognition. In *CVPR*, 2019.
- [43] Yandong Guo, Lei Zhang, Yuxiao Hu, Xiaodong He, and Jianfeng Gao. Ms-celeb-1m: A dataset and benchmark for large-scale face recognition. In *European Conference on Computer Vision*, pages 87–102. Springer, 2016.
- [44] Gary B Huang, Marwan Mattar, Tamara Berg, and Eric Learned-Miller. Labeled faces in the wild: A database for studying face recognition in unconstrained environments. In *Workshop on faces in 'Real-Life' Images: detection, alignment, and recognition*, 2008.
- [45] Ira Kemelmacher-Shlizerman, Steven M Seitz, Daniel Miller, and Evan Brossard. The megaface benchmark: 1 million faces for recognition at scale. In *Proceedings of the IEEE Conference on Computer Vision and Pattern Recognition*, pages 4873–4882, 2016.
- [46] Soumyadip Sengupta, Jun-Cheng Chen, Carlos Castillo, Vishal M Patel, Rama Chellappa, and David W Jacobs. Frontal to profile face verification in the wild. In *2016 IEEE Winter Conference on Applications of Computer Vision (WACV)*, pages 1–9. IEEE, 2016.
- [47] Stylianos Moschoglou, Athanasios Papaioannou, Christos Sagonas, Jiankang Deng, Irene Kotsia, and Stefanos Zafeiriou. Agedb: the first manually collected, in-the-wild age database. In *Proceedings of the IEEE Conference on Computer Vision and Pattern Recognition Workshops*, pages 51–59, 2017.
- [48] Cameron Whitelam, Emma Taborsky, Austin Blanton, Brianna Maze, Jocelyn Adams, Tim Miller, Nathan Kalka, Anil K Jain, James A Duncan, Kristen Allen, et al. Iarpa janus benchmark-b face dataset. In *Proceedings of the IEEE Conference on Computer Vision and Pattern Recognition Workshops*, pages 90–98, 2017.
- [49] Brianna Maze, Jocelyn Adams, James A Duncan, Nathan Kalka, Tim Miller, Charles Otto, Anil K Jain, W Tyler Niggel, Janet Anderson, Jordan Cheney, et al. Iarpa janus benchmark-c: Face dataset and protocol. In *2018 International Conference on Biometrics (ICB)*, pages 158–165. IEEE, 2018.
- [50] K. Zhang, Z. Zhang, Z. Li, and Y. Qiao. Joint face detection and alignment using multitask cascaded convolutional networks. *IEEE Signal Processing Letters*, 23(10):1499–1503, Oct 2016.
- [51] Qiong Cao, Li Shen, Weidi Xie, Omkar M Parkhi, and Andrew Zisserman. Vggface2: A dataset for recognising faces across pose and age. In *2018 13th IEEE International Conference on Automatic Face & Gesture Recognition (FG 2018)*, pages 67–74. IEEE, 2018.
- [52] Weidi Xie and Andrew Zisserman. Multicolumn networks for face recognition. *BMVC*, 2018.
- [53] W. Xie, L. Shen, and A. Zisserman. Comparator networks. In *European Conference on Computer Vision*, 2018.